User Guide for BOD:

Buckling-Restrained Brace and Connection Design Procedures

(Server: S14073101/ Client: C14073101)

Pao-Chun Lin Keh-Chyuan Tsai
An-Chien Wu Ming-Chieh Chuang

National Center for Research on Earthquake Engineering
Department of Civil Engineering, National Taiwan University

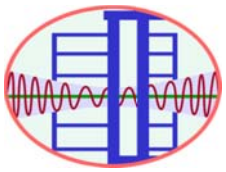

July 2014

PREFACE

The buckling-restrained brace (BRB) has been widely adopted in the past decades because of the cost-effectiveness. The National Center for Research on Earthquake Engineering (NCREE) has completed the seismic tests and the design recommendations for the welded-end slotted BRB (WES-BRB) members and connections [1, 2]. In addition, a cloud service entitled Brace on Demand (BOD) has been developed in NCREE. The designers could conveniently find the detailed design results of WES-BRB member and end connections through the BOD browser (http://BOD.ncree.org.tw). The results of drawings, calculations and spread sheet can be downloaded for preparing the construction document. The users are only required to input the frame geometry, the BRB steel grade and the axial yield force capacity into the BOD browser. Then, the server will perform all the detailed designs, check all the limit states, and output the corresponding WES-BRB dimensions and connection design results using the spreadsheet format. This document introduces complete design procedures and limit states of the WES-BRB member and its connections. It is based on the *Load and Resistance Factor Design* (LRFD) demonstrated in the "*Specification for Structural Steel Buildings*" [3] and "*Seismic Provisions for Structural Steel Buildings*" [4] published by the American Institute of Steel Construction.

CONTENTS

1. THE WES-BRB DESIGN PROCEDURES

(1) Frame Configuration

The dimensional notations of the buckling-restrained braced frame (BRBF) in the diagonal and chevron configurations are shown in Figures 1a and 1b, respectively. The dimensions include the story height (H_{col}), beam span (L_{beam}), left and right column depths ($d_{c,left}$ and $d_{c,right}$), upper and lower beam depths ($d_{b,upper}$ and $d_{b,lower}$) and slab thickness (t_s).

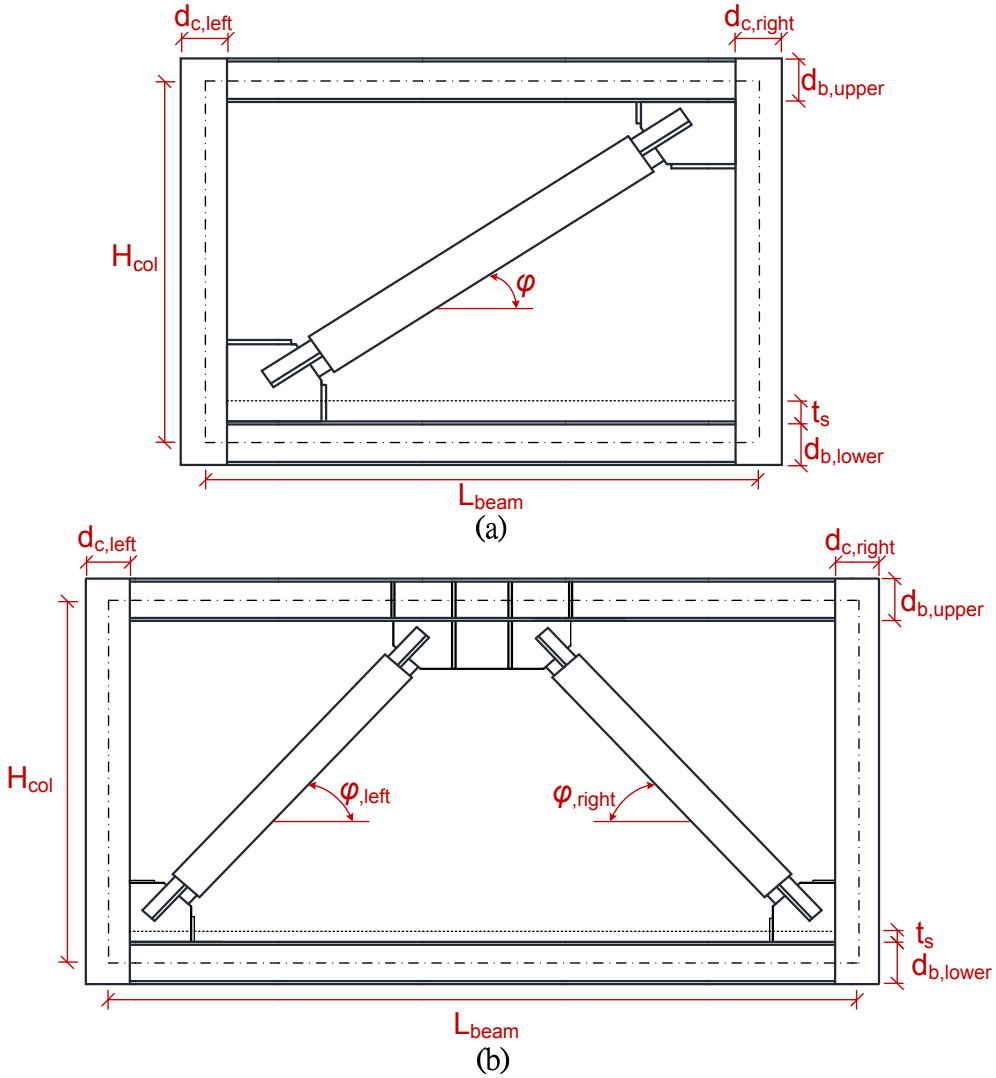

Figure 1. The BRBF with (a) diagonal and (b) chevron configurations.

(2) BRB Steel Core Materials

Table 1 lists the three steel grades incorporated in the BOD program. The steel mechanical properties include the nominal yield stress (F_y), overstrength factor (R_y) and strain hardening factor (Ω_h). The compression strength adjustment factor β set equal to 1.15 in the BOD design procedure.

Table 1. The steel material mechanical properties adopted in BOD.

Steel	F_y (MPa)	R_y	Ω_h	β
ASTM A572 GR50	345	1.1	1.3	1.1~1.2
ASTM A36	248	1.3	1.5	1.1~1.2
CNS SN490B	324	1.2	1.3	1.1~1.2

(3) Maximum BRB Axial Force Capacity

The cross-sectional area of the BRB energy dissipation section (A_c) can be computed according to the steel grade and the nominal yielding strength (P_y) specified by the users:

$$A_c = \frac{P_y}{F_y} \tag{1}$$

The maximum BRB compressive axial force capacity ($P_{\max}$) can be calculated as follows:

$$P_{\max} = P_y \times R_y \times \Omega_h \times \beta \tag{2}$$

The maximum BRB tensile axial force capacity can be computed from $P_{\max} / \beta$.

(4) BRB Cross-sectional Dimensions

It can be found in the "Standard Drawing" in the BOD download, or from Figures 1a, 1b and 2 for details of the WES-BRB cross-sectional dimensions, where, t_c is the thickness of the steel core plate perpendicular to the gusset plate, B_c and D_c are the cross-sectional width and depth of the energy dissipation section, respectively. The t_j is the thickness of the steel core plate parallel to the gusset plate, B_j and D_j are the cross-sectional width and depth of the joint section, respectively. The A_c, A_j and A_t are the cross-sectional areas of the energy dissipation section, the joint section and the transition section, respectively. The A_t can be computed by averaging the A_c and A_j.

As shown in Figure 2, L_{wp} is the distance from work point to work point, L_{BRB} is the total end-to-end length of the BRB component, L_{sc} is the steel casing length, L_c and L_t are the length of the energy dissipation section and transition section, respectively. The L_x is the length of joint section inside the steel casing. The $L_{j,e}$ is the BRB joint end length. The total joint section length $L_{j,wp}$ can be computed as L_{wp}-L_c-2L_t.

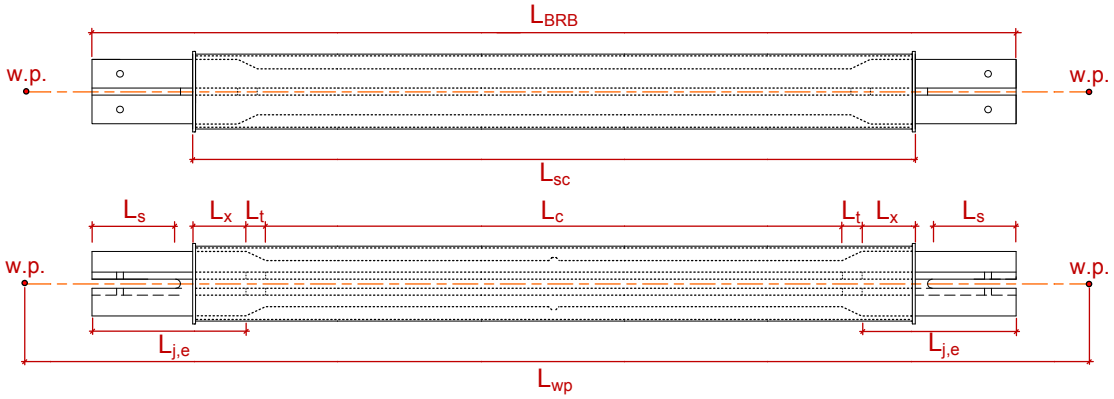

Figure 2. The WES-BRB component.

(5) BRB End-to-Gusset Connection Weld Requirements

The fillet weld length on the BRB-to-gusset connection (L_w) as shown in Figures 3a and 3b can be computed as follows [1]:

$$\begin{aligned} &\phi \times 0.707 \times T_w \times \left(4L_w + D_j\right) \times \left(0.6F_{exx}\right) \geq P_{\max} \\ &\phi = 0.75 \end{aligned} \tag{3}$$

The fillet weld leg size (T_w) equals to 0.8t_c and the weld material strength F_{exx} equals to 490 MPa in the BOD program. The slot length at the core plate ends of the joint section (L_s) is 25 mm longer than L_w (L_s = L_w + 25) and the slot width is 3 mm wider than gusset plate thickness ($t_{g,s}$ = t_g + 3) for the construction site fitting purpose.

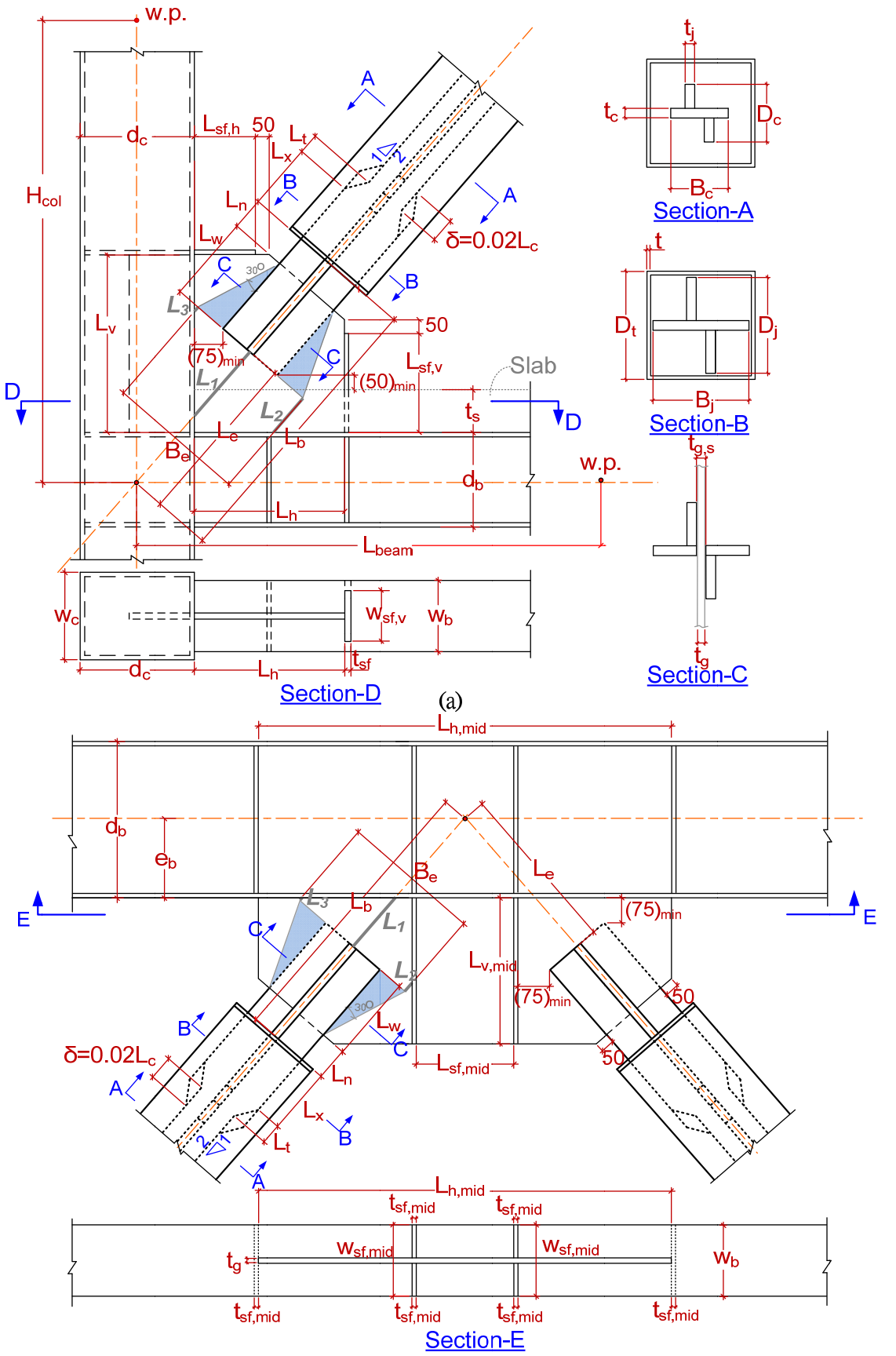

Figure 3. The WES-BRB end-to-gusset connection details of the (a) corner gusset and (b) middle gusset.

(6) BRB Steel Core Dimensions in Joint Section

As shown in Figures 3a and 3b, an additional space of length (δ) near each end of the steel casing is required. Styrofoam is applied in this zone to allow the BRB ends to be compressed without crushing into the infill mortar. The length δ is taken as $0.02L_c$ by assuming the BRB will be compressed to a 4% peak core strain. The distance from the steel casing ends to the edge of gusset plate (L_n) is set to be 25 mm longer than δ ($L_n = \delta + 25$). In addition, L_x is set equal to $2L_n$ in the BOD. L_e is the distance from the BRB end to the work point.

(7) BRB Effective Stiffness

When the BRB deforms into the inelastic ranges, the plastic deformation will concentrate at the energy dissipation section of the steel core. The energy dissipation section length ratio α is defined as follows [1]:

$$\alpha = \frac{L_c}{L_{wp}} \tag{4}$$

As noted above, the steel core joint section slots into the gusset. The beam and column sections will somewhat enlarge the cross-sectional area near the outer end of the joint section. Thus, the cross-sectional area of the joint section in enlarged to $1.2A_j$ for computing the BRB effective stiffness [5]. The effective stiffness of the BRB (K_{eff}) can be computed from the inverse of the sum of three individual flexibilities, the energy dissipation section ($1/K_c$), transition section ($1/K_t$) and joint section ($1/1.2K_j$):

$$K_{eff} = \frac{1}{\frac{1}{K_c} + \frac{1}{K_t} + \frac{1}{1.2K_j}} = \frac{EA_cA_tA_j}{L_cA_tA_j + 2L_tA_cA_j + \frac{L_{j,wp}A_cA_t}{1.2}} \tag{5}$$

where E is the Young's modulus of steel. If the BRBs are represented by truss elements in an analytical model, the length of the truss element can be work point to work point (L_{wp}) distance. The cross-sectional area of the truss element can be taken as the energy dissipation section cross-sectional area (A_c). In order to obtain the corresponding BRB effective stiffness (K_{eff}), the Young's modulus of the truss element must be modified by the effective stiffness factor Q defined as:

$$Q = \frac{K_{eff}}{EA_c / L_{wp}} \tag{6}$$

The value of the Q factor is closely related to the value of α. For a given BRB L_{wp}, the shorter the energy dissipation section length is, the smaller the α value and the larger the Q factor will be. Furthermore, the BRB effective stiffness and the Q factor will increase when the length and cross-sectional area of the transition or joint section are increased. In general, the value of Q factor is ranging from 1.2 to 1.5 for a very long to a very short BRB, respectively. If it is necessary, the BOD users may specify an effective stiffness or the length ratio α. Based on the users' requirements, the BOD will adjust the cross-sectional area and the length of each section. The maximum value of the effective stiffness factor Q acceptable in the BOD is set at 1.6.

(8) Steel Casing

The steel casing of the BRB must be strong enough to prevent the steel core from flexural buckling. Euler buckling strength of the steel casing must be greater than maximum BRB

axial force capacity. Thus, the moment of inertia (I_{sc}) of the steel casing must satisfy [6]:

$$I_{sc} \geq \frac{P_{\max} L_{sc}^{\ 2}}{\pi^2 E} \tag{7}$$

As shown in Figure 2, the steel casing length (L_{sc}) is L_{BRB}-$2L_w$-$2L_n$.

2. GUSSET PLATE DESIGN PROCEDURES

(1) Corner Gusset Plate

For the gusset plate design, the BOD adopts the General Uniform Force Method (GUFM) [7] to compute the gusset-to-beam and gusset-to-column interface forces. The BOD also takes the additional force demands induced by the frame action effect into consideration.

As shown in Figure 4, the GUFM assumes that the gusset-to-beam and gusset-to-column interface forces act at the middle of the gusset plate length (L_h) and height (L_v), respectively. The interface forces and the brace axial force directions pass through the gusset control point to achieve the moment equilibrium. It also assumes that the gusset-to-beam interface force direction passes through the beam control point intersected by the beam center line and column face. Thus, the gusset control point can be determined. Using the static force equilibrium, the gusset-to-beam and gusset-to-column interface forces can be obtained as follows:

$$H_{uc} = \frac{P_{\max} e_c \sin\varphi}{e_b + 0.5L_v} \tag{8}$$

$$V_{ub} = P_{\max}\left[\frac{e_b\left[\left(e_b + 0.5L_v\right)\cos\varphi - e_c \sin\varphi\right]}{0.5L_h\left(e_b + 0.5L_v\right)}\right] \tag{9}$$

$$H_{ub} = P_{\max}\cos\varphi - H_{uc} \tag{10}$$

$$V_{uc} = P_{\max}\sin\varphi - V_{ub} \tag{11}$$

where, V_{uc} and H_{uc} are the vertical and horizontal force components at gusset-to-column interface induced by the BRB axial force, respectively. The V_{ub} and H_{ub} are the vertical and horizontal force components at gusset-to-beam interface induced by the BRB force, respectively. The e_c and e_b are half of the column and beam depths, respectively.

Figure 5 shows the equivalent strut model for the gusset plate considering the frame action effect [8]. The gusset-to-beam and gusset-to-column interface forces can be computed from the axial force in the equivalent strut induced from the beam shear. The strut width is assumed to be equal to the gusset plate thickness (t_g). The strut depth is assumed to be half of the equivalent strut length ($0.5L_g$) [9]. In order to compute the beam shear, the BOD conservatively considers the ultimate state when the beam moments in front of the gusset plate tips reach the flexural capacity as shown in Figures 6a and 6b. Since the beams are required to sustain the substantial axial force ($P_{r,beam}$) induced by the BRB axial deformations, the beam reduced flexural capacity ($M_{r,beam}$) is computed according to the axial force and flexural interaction but without strength reduction factor as follows [3],

$$\text{if} \quad \frac{P_{r,beam}}{P_{n,beam}} \geq 0.2, \quad \frac{P_{r,beam}}{P_{n,beam}} + \frac{8}{9}\left(\frac{M_{r,beam}}{M_{n,beam}}\right) = 1.0$$
$$\text{if} \quad \frac{P_{r,beam}}{P_{n,beam}} < 0.2, \quad \frac{P_{r,beam}}{2P_{n,beam}} + \frac{M_{r,beam}}{M_{n,beam}} = 1.0 \tag{12}$$

where $M_{n,beam}$ is the beam plastic moment and $P_{n,beam}$ is the beam compression capacity assuming the beam is fully laterally supported. The beam axial force ($P_{r,beam}$) can be represented by the horizontal force component of the maximum BRB axial force (P_{max}) as follows,

$$P_{r,beam} = P_{max}\cos\varphi \tag{13}$$

Thus, the corresponding beam shear demand (V_{beam}), no greater than the beam plastic shear capacity ($V_{p,beam}$), can be computed considering the beam clear span L_{clear}, material overstrength ($R_{y,beam}$) factor [8]:

$$V_{beam} = \frac{2(R_{y,beam}M_{r,beam})}{L_{clear}} \leq V_{p,beam} = 0.6R_{y,beam}F_{y,beam}t_w\left(d_b - 2t_f\right) \tag{14}$$

where $F_{y,beam}$ is the yield stress of the beam material, t_w and t_f are the thicknesses of the beam web and flange, respectively. For the single diagonal BRB configuration (Figure 1a), the beam clear span L_{clear} equals to L_{beam}-$0.5d_{c,left}$-$0.5d_{c,right}$-$L_{h,lower}$-$L_{h,upper}$ assuming the frame and brace dimensions in the stories above and below the design target story are identical with the dimensions in the design target story. For the chevron BRB configuration (Figure 1b), the L_{clear} equals to L_{beam}-$0.5d_{c,left}$-$0.5d_{c,right}$-$L_{h,left}$-$L_{h,right}$, where $L_{h,left}$ and $L_{h,right}$ are the left and right corner gusset lengths, respectively.

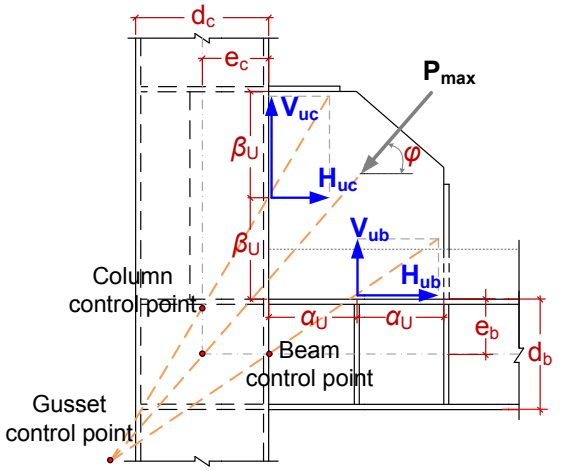

Figure. 4 The gusset-to-beam and gusset-to-column interface force distributions in GUFM.

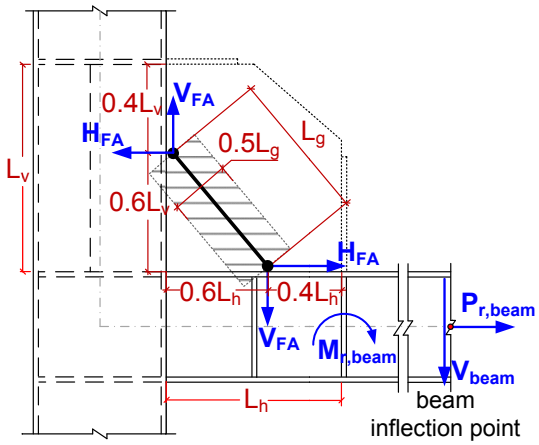

Figure 5. The equivalent strut model for computing force distributions of frame action effect.

Considering the compatibility condition, the horizontal deformation components of the equivalent strut ($d_{strut,x}$) induced by the beam shear and the horizontal deformation component of beam top surface at the location of $0.6L_h$ ($d_{beam,x}$) must be equal. Thus, the equivalent strut horizontal (H_{FA}) and vertical (V_{FA}) force components can be computed [8]:

$$H_{FA} = \frac{d_b L_h V_{beam}\left[0.3\left(L_{beam} - 0.5d_{c,left} - 0.5d_{c,right}\right) - 0.18L_h\right]}{4I_b / t_g + d_b L_h\left(0.3d_b + 0.18L_v\right)} \tag{15}$$

$$V_{FA} = \frac{d_b L_v V_{beam}\left[0.3\left(L_{beam} - 0.5d_{c,left} - 0.5d_{c,right}\right) - 0.18L_h\right]}{4I_b / t_g + d_b L_h\left(0.3d_b + 0.18L_v\right)} \quad (16)$$

As shown in Figure 6a, the BRB is being compressed with the beam-to-column corner open. Considering the combination of brace compressive force and frame action effects, the gusset-to-column horizontal ($H_{c,c}$) and vertical ($V_{c,c}$) force components and the gusset-to-beam vertical ($V_{b,c}$) and horizontal ($H_{b,c}$) force components can be computed:

$$H_{c,c} = H_{FA} - H_{uc} \quad (17)$$

$$V_{c,c} = V_{FA} + V_{uc} \quad (18)$$

$$H_{b,c} = H_{FA} + H_{ub} \quad (19)$$

$$V_{b,c} = V_{FA} - V_{ub} \quad (20)$$

As shown in Figure 6b, the BRB is being tensed with the beam-to-column corner close. Considering the combination of brace tensile force and frame action effects, the gusset-to-column horizontal ($H_{c,t}$) and vertical ($V_{b,t}$) force components and he gusset-to-beam vertical ($V_{b,t}$) and horizontal ($H_{b,t}$) force components can be computed as follows:

$$H_{c,t} = H_{FA} - H_{uc} / \beta \quad (21)$$

$$V_{c,t} = V_{FA} + V_{uc} / \beta \quad (22)$$

$$H_{b,t} = H_{FA} + H_{ub} / \beta \quad (23)$$

$$V_{b,t} = V_{FA} - V_{ub} / \beta \quad (24)$$

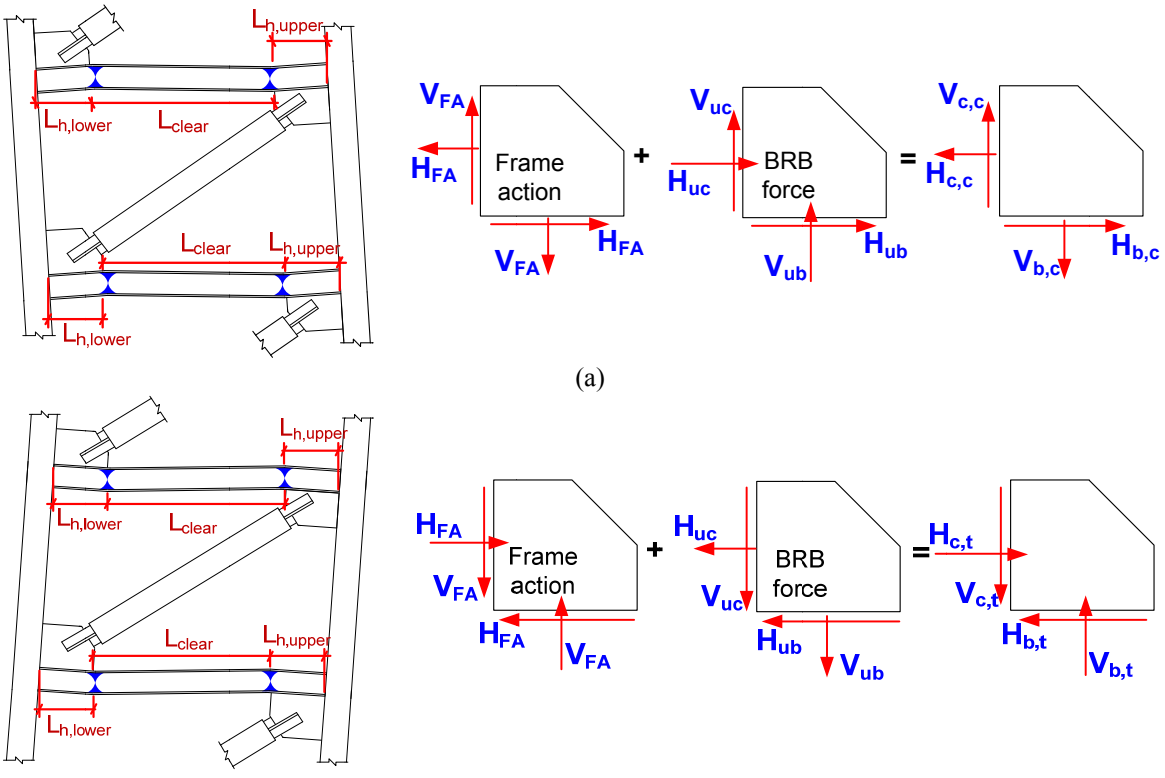

Figure 6. The force distributions on the gusset interfaces with (a) the BRB is compressed when beam-to-column corner open, and (b) BRB is tensed when beam-to-column corner close.

The effectiveness of the aforementioned procedures in computing the corner gusset-to-beam and gusset-to-column interface force demands have been verified by large scale BRBF tests and finite element model analyses [2]. The complete gusset plate design procedures are as follows:

(a) Configure the gusset plate shape and thickness based on the geometry of the BRB connection and the architectural space requirements.

(b) The ASTM A572 GR 50 and CNS SN490B steel materials are recommended for the gusset plate design using the BOD. As shown in Figure 3a, the BOD designs the gusset plate free edges to be either horizontal or vertical.

(c) Calculate the gusset-to-beam and gusset-to-column interface force demands resulted from the BRB by using the GUFM (Equations 8 to 11).

(d) Calculate the gusset-to-beam and gusset-to-column interface force demands resulted from the frame action effect by using the equivalent strut model (Equations 15 to 16).

(e) Calculate the total force demands on the gusset-to-beam and gusset-to-column interfaces by using Equations 17 to 24.

(f) In the BOD, the fillet weld leg size on the gusset-to-beam (T_b) and gusset-to-column (T_c) interfaces will be computed as follows if t_g is less than 20 mm.

$$\phi V_{an,c} \geq 1.25\sqrt{V_{c,c}^2 + H_{c,c}^2} \tag{25}$$

$$\phi V_{an,b} \geq 1.25\sqrt{V_{b,c}^2 + H_{b,c}^2} \tag{26}$$

where, $V_{an,c} = 2\times 0.707 \times T_c L_v \left(0.6F_{exx}\right)\left[1+0.5\sin^{1.5}\left(\tan^{-1}\left|\frac{H_{c,c}}{V_{c,c}}\right|\right)\right]$

$$V_{an,b} = 2\times 0.707 \times T_b L_h \left(0.6F_{exx}\right)\left[1+0.5\sin^{1.5}\left(\tan^{-1}\left|\frac{V_{b,c}}{H_{b,c}}\right|\right)\right]$$

ϕ=0.75

The complete joint penetration weld is adopted on the gusset-to-beam and gusset-to-column interface if the gusset plate thickness is greater than 20 mm.

(g) The gusset edge stiffeners are highly recommended for both the vertical and horizontal free edges of the corner gusset plate. As shown in Figure 3a, the gusset edge stiffener thickness (t_{sf}) is set no greater than 20 mm, but equals to the gusset plate thickness (t_g) when t_g is smaller than 20 mm. The width of the vertical ($w_{sf,v}$) and horizontal ($w_{sf,h}$) gusset edge stiffeners are set equal to the beam flange width but no greater than 300 mm. As illustrated in Figure 3a, the lengths of the vertical and horizontal gusset edge stiffener are $L_{sf,v}$ and $L_{sf,h}$,respectively. The clearances of 50 mm on gusset horizontal and vertical free edges from the cut corner are required for the WES-BRB installation.

(2) Middle Gusset Plate

The middle gusset plate in the V-shape or chevron BRBF configuration is required to transfer the two BRB forces without the frame action effect. However, there is an eccentricity exist between the gusset-to-beam interface weld and the BRBs' work point as shown in Figure 7. Thus, the additional moment demand on the weld must be considered. Assume two BRBs are same size, the gusset-to-beam interface normal compressive force ($V_{b,mid}$), shear force ($H_{b,mid}$) and moment ($M_{b,mid}$) can be computed as follows:

$$V_{b,mid} = P_{\max}\left(1-\frac{1}{\beta}\right)\sin\varphi \tag{27}$$

$$H_{b,mid} = P_{\max}\left(1+\frac{1}{\beta}\right)\cos\varphi \tag{28}$$

$$M_{b,mid} = H_{b,mid}e_b = P_{\max}e_b\left(1+\frac{1}{\beta}\right) \tag{29}$$

The corresponding shear stress ($F_{s,mid}$), maximum tensile ($F_{t,mid}$) and compressive stresses ($F_{c,mid}$) can be computed as follows:

$$F_{s,mid} = \frac{H_{b,mid}}{L_{h,mid}t_g} \tag{30}$$

$$F_{t,mid} = \frac{M_{b.mid}}{L_{h,mid}^2 t_g/4} - \frac{V_{b,mid}}{L_{h,mid}t_g} \tag{31}$$

$$F_{c,mid} = \frac{M_{b.mid}}{L_{h,mid}^2 t_g/4} + \frac{V_{b,mid}}{L_{h,mid}t_g} \tag{32}$$

The strength method described in the model steel building codes [3] is adopted in BOD for the gusset-to-beam interface fillet weld design when the gusset plate thickness is smaller than 20 mm. The fillet welds are divided into several elements as shown in Figure 8. Then the total capacity is computed by summing all he individual weld segment strength. The nominal strength of each individual weld segment (R_i) can be computed as follows:

$$R_i = 2\times 0.707\times T_{b,mid}\left(0.6F_{exx}\right)\left(1+0.5\sin^{1.5}\theta\right)\left[\frac{\Delta_i}{\Delta_m}\left(1.9-0.9\frac{\Delta_i}{\Delta_m}\right)\right]^{0.3}\times\left(\frac{L_{h,mid}}{10}\right) \tag{33}$$

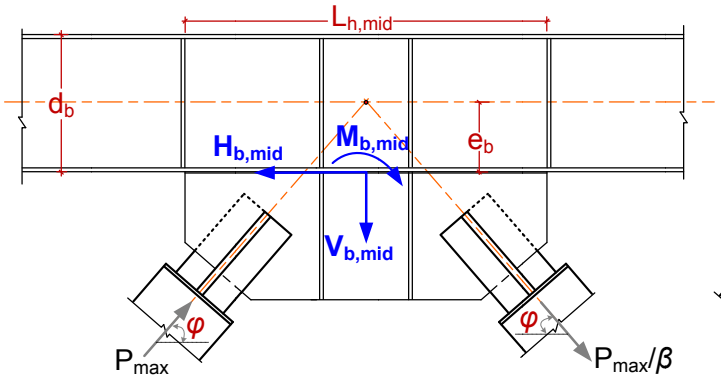

Figure 7. The force distributions of the middle gusset plate.

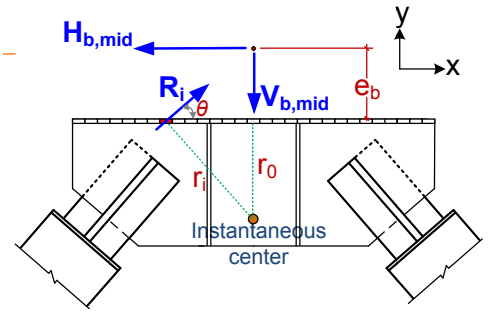

Figure 8. The strength method for the fillet weld design.

θ = angle of loading measured from the weld longitudinal axis, (degrees).

Δ_i = $r_i\left(\frac{\Delta_u}{r_{crit}}\right)$, deformation of element i, (in), where $\left(\frac{\Delta_u}{r_{crit}}\right)$ is the smallest $\frac{\Delta_u}{r}$ among all the segments.

Δ_m = $0.209\left(\theta+2\right)^{-0.32}T_{b,mid}$, deformation of the element at maximum strength, (in).

Δ_u = $1.087(\theta+6)^{-0.65} T_{b,mid} \le 0.17 T_{b,mid}$, deformation of the element when fracture is imminent, usually in the element farthest from instantaneous center of rotation, (in).

$T_{b,mid}$ = Fillet weld leg size on the middle gusset-to-beam interface, (mm).

F_{exx} = the weld material strength, (490 MPa).

The middle gusset design procedures are as follows:

(a) Divide the weld configuration ($L_{h,mid}$) into several segments. The BOD divides the weld into 10 segments for the first iteration.

(b) Select an arbitrary value for $T_{b,mid}$. The BOD adopts 5 mm for the first iteration.

(c) As shown in Figure 8, select trial location of instantaneous center (r_0).

(d) As shown in Figure 8, assume the resisting force R_i at any weld segment acts in a direction perpendicular to the radial line from the instantaneous center to the centroid of the weld segment.

(e) Compute the angle θ (degree) between the direction of the resisting force R_i and the axis of weld.

(f) Compute the deformations Δ_m and Δ_u which can occur at the particular θ of the weld segment.

(g) Deformations on weld segments are assumed to vary linearly with the distance from the instantaneous center to the centroid of the weld segment. Thus, the critical segment is the one where the ratio of its Δ_u to its radial distance r_i is the smallest.

(h) Compatible deformations Δ_i are then computed at each weld segment.

(i) Compute the nominal strength R_i of each weld segment.

(j) Using statics, compute the load P_n that represents the nominal strength of the connection when the load is applied at the given eccentricity e_b:

$$\sum M = 0, \quad P_n(e_b + r_0) = \sum R_i r_i$$
$$\sum F_y = 0, \quad P_n = \sum R_{i,y}$$

(k) Compare the values of P_n from the above two equations, if they are equal the solution is correct. If they are not equal, revise the trial value of r_0 and repeat the process.

(l) Once the value of r_0 is correctly chosen, recalculate the P_n to meet the following equations by using appropriate weld size $T_{b,mid}$:

$$\phi P_{n,x} \ge H_{b,mid}$$
$$\phi P_{n,y} \ge V_{b,mid}$$
$$\phi = 0.75$$

If the middle gusset plate thickness is greater than 20 mm, the complete joint penetration weld is adopted for the gusset-to-beam interface welding. The gusset plate stiffeners are required to maintain the out-of-plan stability of the gusset plate. As shown in Figure 3b, the gusset stiffeners are required to satisfy the following requirements:

(a) The stiffener thickness ($t_{sf,mid}$) is equal to the middle gusset plate thickness (t_g) but should be no greater than 20 mm.
(b) The outer edge-to-outer edge width of the stiffener ($w_{sf,mid}$) is the same as the beam flange width (w_b).
(c) As shown in Figure 3b, a clear distance of 75 mm is required between the BRB ends to the beam flange bottom surface and gusset stiffener. The clear distance between the two gusset stiffeners ($L_{sf,mid}$) should be greater than half of the middle gusset plate height ($L_{sf,mid} \geq 0.5L_{v,mid}$).
(d) If the clear distance between the two gusset stiffeners ($L_{sf,mid}$) is smaller than $0.5L_{v,mid}$ when the aforementioned 75 mm clear distance requirement is satisfied, then the gusset stiffeners are adopted only at the middle of the gusset plate as shown in Figure 9.
(e) Additional beam web stiffeners with sufficient width and a thickness same as the gusset stiffener ($t_{sf,mid}$) are required at the gusset tips and locations align with the gusset stiffeners as shown in Figure 3b and 9.

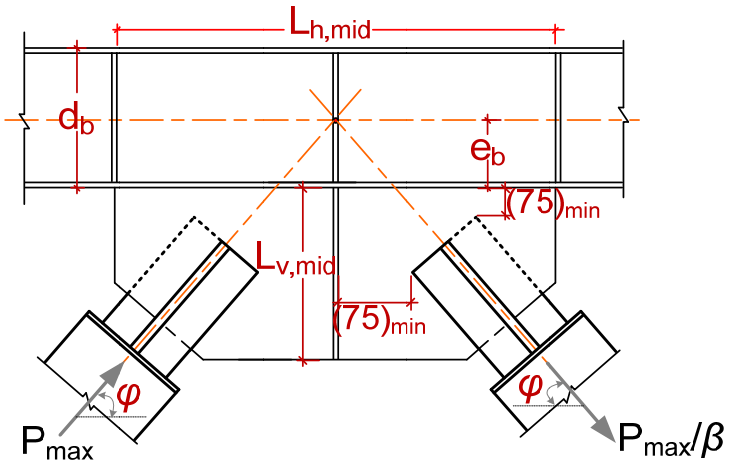

Figure 9. The middle gusset plate with single stiffener.

3. DESIGN DEMAND-TO-CAPACITY RATIO (DCR) CHECKS

(1) Steel Casing Buckling (DCR-1)

Check the steel casing to prevent the steel core from flexural buckling using Equation 7.

(2) Joint Region Yielding (DCR-2)

$$\phi A_j F_y R_y \geq P_{\max} / \beta$$
$$\phi = 0.90 \tag{34}$$

(3) Joint Region Buckling (DCR-3)

$$\phi P_{cr,upper} = \phi \times \min\left[\frac{\pi^2 EI_{yj}}{4\left(L_{b,upper} + \delta\right)^2}, A_j F_y R_y\right] \geq P_{\max} \tag{35}$$

$$\phi P_{cr,lower} = \phi \times \min\left[\frac{\pi^2 EI_{yj}}{4\left(L_{b,lower} + \delta\right)^2}, A_j F_y R_y\right] \geq P_{\max} \tag{36}$$

$$\phi = 0.90$$

where, I_{yj} is the moment of inertia of the joint section in the gusset out-of-plan direction. $L_{b,upper}$ and $L_{b,lower}$ are the distances from the work points to the steel casing upper and lower ends, respectively.

(4) Gusset Plate Block Shear Failure (DCR-4)

$$\phi P_n \geq P_{\max} \tag{37}$$

in which, $P_n = 0.6F_{u,g}A_{nv} + F_{u,g}A_{nt} \leq 0.6F_{y,g}A_{gv} + F_{u,g}A_{nt}$, $\phi = 0.75$.

As shown in Figures 3a, 3b and 10, the sectional area under the tension is $A_{gt}=A_{nt}=D_j \times t_g$, the sectional area under the shear is $A_{gv}=A_{nv}=2L_w \times t_g$. $F_{y,g}$ and $F_{u,g}$ are the yield stress and tensile strength of the gusset steel.

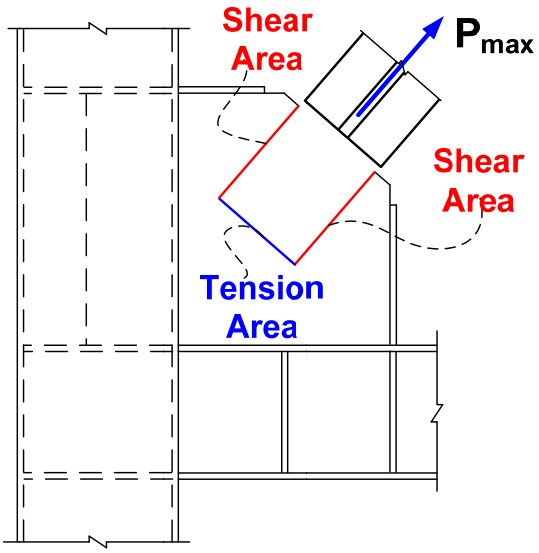

Figure 10. The block shear failure of the BRB end-to-gusset connection.

(5) Gusset Plate Yielding (DCR-5)

The capacity of the gusset plate responsible for transferring the BRB tension can be computed by calculating the yielding capacity of the Whitmore section on the gusset plate [10]. The Whitmore section region is determined by extending the BRB end-to-gusset weld pattern at a 30-degree angle as shown in Figure 3a. The Whitmore section width $W_{whitmore}$ can be computed as follows:

$$W_{whitmore} = 2L_w \times \tan 30^\circ + D_j \tag{38}$$

The gusset yielding capacity can be calculated using the effective section width B_e, the smaller dimension of $W_{whitmore}$ or W_{actual} as shown in Figures 3a and 3b. If the Whitmore section goes beyond the actual gusset plate region, the W_{actual} considering the intersection of the gusset plate and the Whitmore section is adopted. The gusset plate yielding capacity can be computed as follows:

$$\phi F_{y,g} B_e t_g \geq P_{\max} / \beta \tag{39}$$
$$\phi = 0.90$$

(6) Gusset Plate Buckling (DCR-6)

The gusset plate compressive strength can be computed by adopting the width B_e and the average of the three critical lengths as the buckling length (L_r). The critical lengths L_1, L_2 and L_3 can be determined as shown in Figures 3a and 3b. If one of the ends of the width B_e

inserts with the beam or column face, the corresponding critical length is negative. The buckling length L_r is computed from:

$$L_r = \frac{L_1 + L_2 + L_3}{3} \tag{40}$$

The gusset plate compressive strength can be computed from the following equation:

$$\phi \times P_{cr,g} = \phi \times \left(B_e \times t_g \right) \times F_{cr,g} \geq P_{\max} \tag{41}$$

if $\lambda_c \leq 1.5$, $F_{cr,g} = 0.658^{\lambda_c^2} F_{y,g}$

if $\lambda_c > 1.5$, $F_{cr,g} = \frac{0.877}{\lambda_c^2} F_{y,g}$

where $\lambda_c = \frac{KL_r}{\pi r}\sqrt{\frac{F_{y,g}}{E}}$, K equals to 0.65 [11,12].

$\phi = 0.90$

(7) Gusset Strength at the Connections to the Beam and Column

(a) von Mises Yield Criterion (DCR-7-1 and DCR-7-4)#

The maximum von Mises stress computed from the normal and shear stress under the maximum brace axial force and frame action effect must be no greater than the yield stress of the gusset plate material. The following requirements are considered:

$$\sqrt{\left(\frac{H_{c,c}}{L_v t_g + w_{sf,eff} t_{sf}} \right)^2 + 3\left(\frac{V_{c,c}}{L_v t_g + w_{sf,eff} t_{sf}} \right)^2} \leq \phi F_{y,g} \tag{42}$$

$$\sqrt{\left(\frac{V_{b,c}}{L_h t_g + w_{sf,eff} t_{sf}} \right)^2 + 3\left(\frac{H_{b,c}}{L_h t_g + w_{sf,eff} t_{sf}} \right)^2} \leq \phi F_{y,g} \tag{43}$$

$\phi = 1.00$

Partial cross-sectional area of the gusset edge stiffener could be taken into account for the gusset-to-beam and gusset-to-column interface area. The effective width of the gusset edge stiffener ($w_{sf,eff}$) should be $2.5t_g$. The von Mises yield criterion for the middle gusset-to-beam interface should satisfy the following requirement:

$$\sqrt{\left(\frac{V_{b,mid}}{L_{h,mid} t_g} + \frac{M_{b,mid}}{L_{h,nid}^2 t_g / 4} \right)^2 + 3\left(\frac{H_{b,mid}}{L_{h,mid} t_g} \right)^2} \leq \phi F_{y,g} \tag{44}$$

$\phi = 1.00$

(b) Tensile Rupture (DCR-7-2 and DCR-7-5)

As illustrated in Figure 6, when the gusset-to-column interface force $H_{c,c} < 0$ or $H_{c,t} > 0$ and the gusset-to-beam interface force $V_{b,c} < 0$ or $V_{b,t} > 0$, these indicate that the corresponding interfaces are subjected to tensile force. The tensile rupture strength at the gusset-to-beam and gusset-to-column interfaces must satisfy the following requirements:

$$H_{c,c} \geq 0 \quad , \quad \frac{H_{c,c}}{L_v t_g + w_{sf,eff} t_{sf}} \leq \phi F_{u,g} \tag{45}$$

$$H_{c,t} \leq 0 \quad , \quad \left| \frac{H_{c,t}}{L_v t_g + w_{sf,eff} t_{sf}} \right| \leq \phi F_{u,g} \tag{46}$$

$$V_{b,c} \geq 0 \quad , \quad \frac{V_{b,c}}{L_h t_g + w_{sf,eff} t_{sf}} \leq \phi F_{u,g} \tag{47}$$

$$V_{b,t} \leq 0 \quad , \quad \left| \frac{V_{b,t}}{L_h t_g + w_{sf,eff} t_{sf}} \right| \leq \phi F_{u,g} \tag{48}$$

where, $w_{sf,eff} = 2.5t_g$, only a limited width of the edge stiffeners is considered. The middle gusset-to-beam interface rupture strength must satisfy the following requirement:

$$F_{t,mid} = \frac{M_{b.mid}}{L_{h,mid}^2 t_g / 4} - \frac{V_{b,mid}}{L_{h,mid} t_g} \leq \phi F_{u,g} \tag{49}$$

ϕ=0.75

(c) Shear Rupture (DCR-7-3 and DCR-7-6)

$$\frac{V_{c,c}}{L_v t_g + w_{sf,eff} t_{sf}} \leq \phi \tau_{u,g} = \phi\left(0.6F_{u,g}\right) \tag{50}$$

$$\frac{H_{b,c}}{L_h t_g + w_{sf,eff} t_{sf}} \leq \phi \tau_{u,g} = \phi\left(0.6F_{u,g}\right) \tag{51}$$

where, $w_{sf,eff} = 2.5t_g$. The middle gusset-to-beam interface must satisfy the following requirement:

$$F_{s,mid} = \frac{H_{b,mid}}{L_{h,mid} t_g} \leq \phi \tau_{u,g} = 0.6\phi F_{u,g} \tag{52}$$

ϕ=0.75

REFERENCES

1. Tsai KC, Wu AC, Wei CY, Lin PC, Chuang MC and Yu YJ, 2014, "Welded end-slot connection and debonding layers for buckling-restrained braces," Earthquake Engineering and Structural Dynamics, DOI: 10.1002/eqe.2423.
2. Lin PC, Tsai KC, Wu AC and Chuang MC, 2014, "Seismic design and test of gusset connections for buckling-restrained brace frames," Earthquake Engineering and Structural Dynamics, Vol. 43, Issue 4, pp. 565-587.
3. American Institute of Steel Construction (AISC), 2010, "Specification for Structural Steel Buildings", Chicago, Illinois.
4. American Institute of Steel Construction (AISC), 2010, "Seismic Provisions for Structural Steel Buildings", Chicago, Illinois.
5. Yu YJ, Tsai KC, Li CH, Weng YT and Tsai CY, 2013, "Earthquake responses analyses of a full-scale five-story steel frame equipped with two types of dampers,"Earthquake Engineering and Structural Dynamics, Vol. 42, Issue 8, pp.

1301-1320.

6. Watanabe A, Hitomi Y, Saeki E, Wada A and Fujimoto M, 1988, "Properties of braces encased in buckling-restraining concrete and steel tube," Proceedings of the 9th World Conference on Earthquake Engineering, Vol. IV, pp. 719-724, Tokyo-Kyoto, Japan.
7. Muir S, 2008, "Design compact gussets with the uniform force method." Engineering Journal, 1st quarter.
8. Lee CH, 2002, "Seismic design of rib-reinforced steel moment connections based on equivalent strut model." Journal of Structural Engineering, pp. 1121-1129.
9. Kaneko K, Kasai K, Motoyui S, Sueoka T, Azuma Y, Ooki Y, 2008, "Analysis of beam-column-gusset components in 5-story value-added frame." the 14th world conference on Earthquake Engineering.
10. Whitmore RE. Experimental investigation of stresses in gusset plate. University of Tennessee Engineering Experiment Station Bulletin No. 16, May 1952.
11. Tsai KC, Hsiao PC, Wang KJ, Weng YT, Lin ML, Lin KC, Chen CH, Lai JW and Lin SL, 2008, "Pseudo-dynamic tests of a full-scale CFT/BRB frame–Part I: Specimen design, experiment and analysis," Earthquake Engineering and Structural Dynamics, Vol. 37, Issue 7, pp. 1081-1098.
12. Tsai KC and Hsiao PC, 2008, "Pseudo-dynamic tests of a full-scale CFT/BRB frame–Part II: Seismic performance of buckling-restrained braces and connections," Earthquake Engineering and Structural Dynamics, Vol. 37, Issue 7, pp. 1099-1115.

Table for DCRs and Design Checks

DCRs		Diagonal		Chevron				
		Upper	Lower	Left		Middle	Right	
				Upper	Lower		Upper	Lower
DCR-1	Steel Casing Buckling	DCR-1		DCR-1 left		-	DCR-1 right	
DCR-2	Joint Region Yielding	DCR-2		DCR-2 left		-	DCR-2 right	
DCR-3	Joint Region Buckling	DCR-3 upper	DCR-3 lower	DCR-3 left upper	DCR-3 left lower	-	DCR-3 right upper	DCR-3 right lower
DCR-4	Gusset Plate Block Shear Failure	DCR-4		DCR-4 left		-	DCR-4 right	
DCR-5	Gusset Plate Yielding	DCR-5 upper	DCR-5 lower	DCR-5 left upper	DCR-5 left lower	-	DCR-5 right upper	DCR-5 right lower
DCR-6	Gusset Plate Buckling	DCR-6 upper	DCR-6 lower	DCR-6 left upper	DCR-6 left lower	-	DCR-6 right upper	DCR-6 right lower
DCR-7-1	Gusset Strength at the Connection to the Beam – von Mises Yield Criterion	DCR-7-1 upper	DCR-7-1 lower	DCR-7-1 left		DCR-7-1 mid	DCR-7-1 right	
DCR-7-2	Gusset Strength at the Connection to the Beam – Tensile Rupture	DCR-7-2 upper	DCR-7-2 lower	DCR-7-2 left		DCR-7-2 mid	DCR-7-2 right	
DCR-7-3	Gusset Strength at the Connection to the Beam – Shear Rupture	DCR-7-3 upper	DCR-7-3 lower	DCR-7-3 left		DCR-7-3 mid	DCR-7-3 right	
DCR-7-4	Gusset Strength at the Connection to the Column – von Mises Yield Criterion	DCR-7-4 upper	DCR-7-4 lower	DCR-7-4 left		-	DCR-7-4 right	
DCR-7-5	Gusset Strength at the Connection to the Column – Tensile Rupture	DCR-7-5 upper	DCR-7-5 lower	DCR-7-5 left		-	DCR-7-5 right	
DCR-7-6	Gusset Strength at the Connection to the Column – Shear Rupture	DCR-7-6 upper	DCR-7-6 lower	DCR-7-6 left		-	DCR-7-6 right	

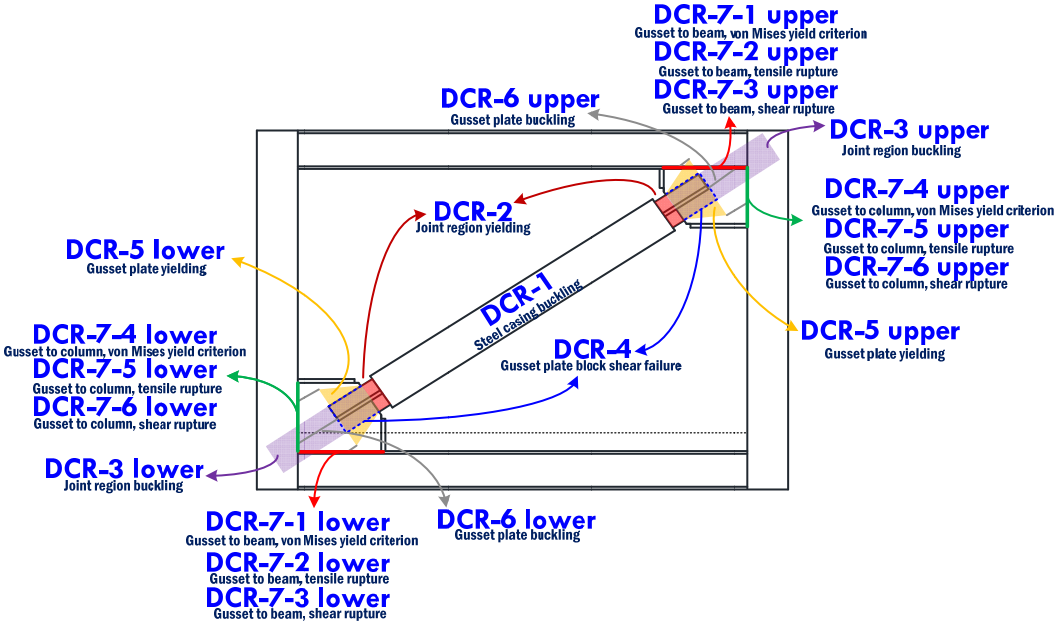

Diagonal Configuration

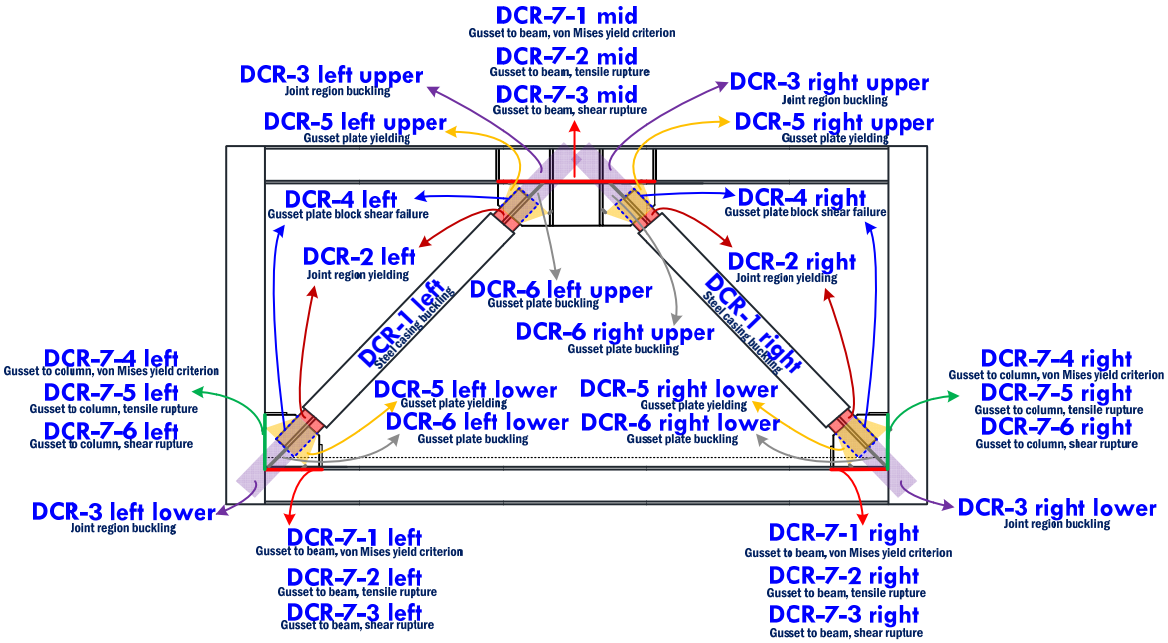

Diagonal Configuration

Table for Notations

Notations of frame		Location			
		Upper	Lower	Left	Right
d_b	Beam depth	$d_{b,upper}$	$d_{b,lower}$	-	-
d_c	Column depth	-	-	$d_{c,left}$	$d_{c,right}$
e_b	Half of beam depth	$e_{b,upper}$	$e_{b,lower}$	-	-
e_c	Half of column depth	-	-	$e_{c,left}$	$e_{c,right}$
H_{col}	Story height	H_{col}			
L_{beam}	Beam span	L_{beam}			
t_s	Slab thickness	t_s			
w_b	Beam width	$w_{b,upper}$	$w_{b,lower}$	-	-
w_c	Column depth	-	-	$w_{c,left}$	$w_{c,right}$

Notations of BRB		Diagonal		Chevron			
		Upper	Lower	Left		Right	
				Upper	Lower	Upper	Lower
A_c	Energy dissipation section cross-sectional area	A_c					
A_j	Joint section cross-sectional area	A_j		$A_{j,left}$		$A_{j,right}$	
A_t	Transition section cross-sectional area	A_t		$A_{t,left}$		$A_{t,right}$	
B_c	Energy dissipation section cross-sectional width	B_c					
B_j	Joint section cross-sectional width	B_j		$B_{j,left}$		$B_{j,right}$	
D_c	Energy dissipation section cross-sectional depth	D_c					
D_j	Joint section cross-sectional depth	D_j		$D_{j,left}$		$D_{j,rigth}$	
L_b	Distance from work point to steel casing end	$L_{b,upper}$	$L_{b,lower}$	$L_{b,leftupper}$	$L_{b,leftlower}$	$L_{b,rightpper}$	$L_{b,rightlower}$
L_{BRB}	BRB end-to-end length	L_{BRB}		$L_{BRB,left}$		$L_{BRB,right}$	
L_c	Energy dissipation section length	L_c		$L_{c,left}$		$L_{c,right}$	
L_e	Distance from BRB end to work point	$L_{e,upper}$	$L_{e,lower}$	$L_{e,leftupper}$	$L_{e,leftlower}$	$L_{e,rightpper}$	$L_{e,rightlower}$
$L_{j,e}$	Joint end length	$L_{j,e}$		$L_{j,e,left}$		$L_{j,e,rigth}$	
$L_{j,wp}$	Joint section length	$L_{j,wp}$		$L_{j,wp,left}$		$L_{j,wp,rigth}$	
L_n	Distance from the steel casing ends to the edge of gusset plate	L_n		$L_{n,left}$		$L_{n,right}$	
L_s	Slot length at the core plate ends of joint section	L_s		$L_{s,left}$		$L_{s,right}$	
L_{sc}	Steel casing length	L_{sc}		$L_{sc,left}$		$L_{sc,rigth}$	
L_t	Transition section length	L_t		$L_{t,left}$		$L_{t,right}$	
L_w	Fillet weld length on BRB end-to-gusset connection	L_w		$L_{w,left}$		$L_{w,right}$	
L_{wp}	Distance from work point to work point	L_{wp}					
t_c	thickness of steel core plate perpendicular to the gusset plate	t_c					
t_j	thickness of steel core plate parallel to the gusset plate	t_j					
T_w	Fillet weld leg size on BRB-to-gusset connection	T_w		$T_{w,left}$		$T_{w,right}$	
δ	Length of space for BRB to be compressed	δ		$\delta_{,left}$		$\delta_{,right}$	
φ	BRB incline angle	φ					

Notations of gusset plate		Diagonal		Chevron		
		Upper	Lower	Left	Middle	Right
L_h	Gusset plate length	$L_{h,upper}$	$L_{h,lower}$	$L_{h,left}$	$L_{h,mid}$	$L_{h,right}$

$L_{sf,mid}$	Clear distance between the two stiffener of middle gusset plate	-	-	-	$L_{sf,mid}$	-
$L_{sf,h}$	Horizontal gusset edge stiffener length	$L_{sf,h,upper}$	$L_{sf,h,lower}$	$L_{sf,h,left}$	-	$L_{sf,h,right}$
$L_{sf,v}$	Vertical gusset edge stiffener length	$L_{sf,v,upper}$	$L_{sf,v,lower}$	$L_{sf,v,left}$	-	$L_{sf,v,right}$
L_v	Gusset plate height	$L_{v,upper}$	$L_{v,lower}$	$L_{v,left}$	$L_{v,mid}$	$L_{v,right}$
T_b	Fillet weld leg size on gusset-to-beam interface	$T_{b,upper}$	$T_{b,lower}$	$T_{b,left}$	$T_{b,mid}$	$T_{b,right}$
T_c	Fillet weld leg size on gusset-to-column interface	$T_{c,upper}$	$T_{c,lower}$	$T_{c,left}$	-	$T_{c,right}$
t_g	Gusset plate thickness	t_g				
t_{sf}	Gusset (edge) stiffener thickness	t_{sf}	t_{sf}	t_{sf}	$t_{sf,mid}$	t_{sf}
$w_{sf,eff}$	Gusset edge stiffener effective width	$w_{sf,eff}$				
$w_{sf,h}$	Horizontal gusset edge stiffener width	$w_{sf,h,upper}$	$w_{sf,h,lower}$	$w_{sf,h,left}$	-	$w_{sf,h,right}$
$w_{sf,mid}$	Outer edge-to-outer edge width of middle gusset stiffener	-	-	-	$w_{sf,mid}$	-
$w_{sf,v}$	Vertical gusset edge stiffener width	$w_{sf,v,upper}$	$w_{sf,v,lower}$	$w_{sf,v,left}$	-	$w_{sf,v,right}$